

**Residue-Based Program of a  $\beta$ -Peptoid Twisted Strand  
Shape via a Cyclopentane Constraint**

Journal:	<i>Organic &amp; Biomolecular Chemistry</i>
Manuscript ID	OB-COM-07-2022-001300.R1
Article Type:	Communication
Date Submitted by the Author:	15-Aug-2022
Complete List of Authors:	Kim, Jungyeon; The University of Tokyo Kobayashi, Hiroka; The University of Tokyo Yokomine, Marin; The University of Tokyo Shiratori, Yota; The University of Tokyo Ueda, Takumi; The University of Tokyo Takeuchi, Koh; The University of Tokyo Umezawa, Koji; Shinshu University Kuroda, Daisuke; The University of Tokyo Tsumoto, Kouhei; The University of Tokyo Morimoto, Jumpei; The University of Tokyo Sando, Shinsuke; The University of Tokyo

## ARTICLE

Residue-Based Program of a  $\beta$ -Peptoid Twisted Strand Shape via a Cyclopentane Constraint

Received 00th January 20xx,  
Accepted 00th January 20xx

DOI: 10.1039/x0xx00000x

Jungyeon Kim,<sup>†a</sup> Hiroka Kobayashi,<sup>a</sup> Marin Yokomine,<sup>a</sup> Yota Shiratori,<sup>b</sup> Takumi Ueda,<sup>c</sup> Koh Takeuchi,<sup>c</sup> Koji Umezawa,<sup>d,e</sup> Daisuke Kuroda,<sup>a,b</sup> Kouhei Tsumoto,<sup>a,b,f</sup> Jumpei Morimoto,<sup>\*a</sup> and Shinsuke Sando<sup>\*a,b</sup>

*N*-Substituted peptides, such as peptoids and  $\beta$ -peptoids, have been reported to have unique structures with diverse functions, like catalysis and manipulation of biomolecular functions. Recently, the preorganization of monomer shape by restricting bond rotations about all backbone dihedral angles has been demonstrated to be useful for de novo design of peptoid structures. Such design strategies are hitherto unexplored for  $\beta$ -peptoids; to date, no preorganized  $\beta$ -peptoid monomers have been reported. Here, we report the first design strategy for  $\beta$ -peptoids, in which all four backbone dihedral angles ( $\omega$ ,  $\phi$ ,  $\theta$ ,  $\psi$ ) are rotationally restricted on a per-residue basis. The introduction of a cyclopentane constraint realized the preorganized monomer structure and led to a  $\beta$ -peptoid with a stable twisted strand shape.

## Introduction

Synthetic oligomers that adopt unique folded structures serve as useful tools that can mimic or improve the functions of biopolymers, such as peptides and proteins. Oligoamides are particularly important among synthetic oligomers owing to their synthetic modularity. Several synthetic oligoamides with well-defined shapes have been reported, e.g.,  $\beta$ -peptides,<sup>1,2</sup>  $\alpha,\alpha$ -disubstituted  $\alpha$ -peptides,<sup>3</sup> aromatic oligoamides,<sup>4–6</sup> AApeptides,<sup>7–9</sup> and peptoids.

Oligo(*N*-substituted glycines) or peptoids,<sup>10</sup> are unique among the synthetic oligoamides owing to the absence of amide hydrogens derived from the *N*-substituted structures. Consequently, the backbone hydrogen bonds cannot be recruited for peptoid folding. Therefore, other intramolecular interactions participate to realize the well-defined structures of peptoids. To this end, strategies using *N*-substituents that introduce intramolecular interactions to peptoids have been developed, including steric effects, electronic interactions, and hydrogen bonds between side chains and backbone.<sup>11–19</sup> These interactions are useful for locally restricting bond rotations about  $\omega$  angles. The local bond restrictions assist

cooperative folding of global peptoid structures into various shapes, such as helices, ribbons, and a loop.<sup>11,12,14–16,20–23</sup> Their unique folding principles enable peptoids to form diverse three-dimensional structures including those that are absent in natural peptides and proteins.<sup>24</sup>

Local restriction of bond rotations about not only  $\omega$  angle but also other backbone dihedral angles facilitates generation of peptoids with defined shapes. Gorske and coworkers reported a design of *N*-substituents that enables per-residue control of two backbone dihedral angles, i.e.,  $\omega$  and  $\phi$  angles.<sup>25,26</sup> The rotational restrictions of multiple backbone dihedral angles improved the predictability of peptoid three-dimensional structures and the designability of new oligomer shapes.

Recently, we reported the first per-residue program of all the backbone dihedral angles of peptoids:  $\phi$ ,  $\psi$ , and  $\omega$  (Fig. 1a).<sup>27</sup> We found that *N*-substituted alanine (NSA) residue is a preorganized peptoid monomer and its oligomers stably form a defined shape determined by the preorganized monomer shape. Because of the residue-based preorganization, oligo-NSA can form a highly stable and predictable shape. The stable and predictable three-dimensional structure of oligo-NSA is beneficial for designing functional molecules like protein ligands.<sup>28,29</sup> Expansion of the repertoire of such preorganized monomers could contribute to the preparation of diverse peptoid shapes of high stability and predictability.

The introduction of another carbon unit into the peptoid backbone using  $\beta$ -amino acids is a promising strategy for expanding the shape diversity of peptoids. Oligo(*N*-substituted  $\beta$ -alanines), referred to as  $\beta$ -peptoid, was first reported in 1998 as a new class of peptoids.<sup>30</sup> Compared to  $\beta$ -amino acid-based peptoids, it is challenging to realize well-defined shapes of  $\beta$ -peptoids due to the existence of an additional rotatable bond compared with  $\alpha$ -amino acid-based peptoids.<sup>31–33</sup> Olsen and coworkers have devised a molecular design of  $\beta$ -peptoids with restricted bond rotations about  $\omega$  (Fig. 1b left).<sup>34</sup> We have previously reported another molecular design of  $\beta$ -peptoids with restricted bond rotations about  $\omega$  and  $\phi$  (Fig. 1b right).<sup>35</sup> Both of the strategies yielded unique crystal

<sup>a</sup> Department of Chemistry and Biotechnology, Graduate School of Engineering, The University of Tokyo, 7-3-1 Hongo, Bunkyo-ku, Tokyo, 113-8656 (Japan). E-mail: jmorimoto@chembio.t.u-tokyo.ac.jp; ssando@chembio.t.u-tokyo.ac.jp

<sup>b</sup> Department of Bioengineering, Graduate School of Engineering, The University of Tokyo, 7-3-1 Hongo, Bunkyo-ku, Tokyo, 113-8656 (Japan)

<sup>c</sup> Graduate School of Pharmaceutical Sciences, The University of Tokyo, 7-3-1 Hongo, Bunkyo-ku, Tokyo, 113-0033 (Japan)

<sup>d</sup> Department of Biomedical Sciences, Graduate School of Science and Technology, Shinshu University, Minaminowa, Nagano 390-8621, Japan

<sup>e</sup> Institute for Biomedical Sciences, Interdisciplinary Cluster for Cutting Edge Research, Shinshu University, Shinshu University, Matsumoto, Nagano 390-8621, Japan

<sup>f</sup> Institute of Medical Science, The University of Tokyo, 4-6-1 Shirokanedai, Minato-ku, Tokyo 108-8639, Japan

<sup>†</sup> Present address: Departments of Chemistry, Pohang University of Science and Technology (POSTECH), Pohang 37673, South Korea

Electronic Supplementary Information (ESI) available: [details of any supplementary information available should be included here]. See DOI: 10.1039/x0xx00000x

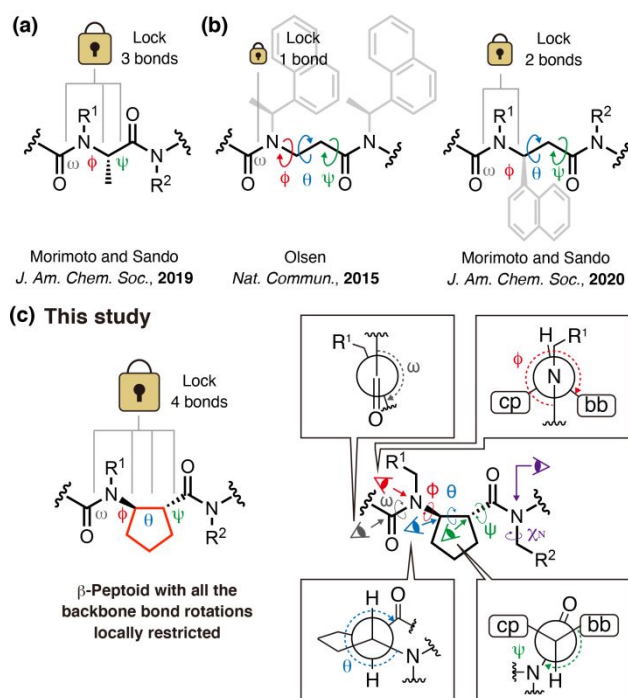


**Fig. 1** (a) Peptoid with all three backbone bonds rotationally restricted. (b)  $\beta$ -Peptoids with one or two backbone bonds rotationally restricted. (c)  $\beta$ -Peptoid with all four backbone bond rotations restricted (this study). The definition of each dihedral angle of the  $\beta$ -peptoid is shown on the right. The dotted arrows indicate the directions of the angles with positive values. “bb” denotes “backbone” and “cp” denotes “cyclopentane”.

structures of  $\beta$ -peptoids that have not been found in peptoids with  $\alpha$ -amino acid backbones, which demonstrated the potential of  $\beta$ -peptoids to expand the oligomer shape diversity of peptoid-type oligomers. However, not all the backbone dihedral angles in these  $\beta$ -peptoids are restricted in rotation. Molecular dynamics (MD) simulations of these structures suggested that their conformations dynamically change at the time scale of nanoseconds to microseconds.

Here, we report the first  $\beta$ -peptoid monomer, in which all the backbone dihedral angles are rotationally restricted on a per-residue basis. A cyclopentane constraint was introduced on the  $\beta$ -peptoid backbone to restrict the backbone bond rotations, which led to per-residue rotational restrictions of all the backbone dihedral angles of the  $\beta$ -peptoids (Fig. 1c). This led to  $\beta$ -peptoids with a predictable and well-defined twisted strand shape.

## Results and Discussion

We hypothesized that introducing cyclopentane constraints will restrict all the backbone bond rotations. We considered (1*R*,2*R*)-2-aminocyclopentanecarboxylic acid (*trans*-ACPC) as a representative backbone with a cyclopentane constraint (Fig. 1c left). As has been elegantly shown by Gellman and coworkers previously, a cyclopentane ring rigidifies the structures of  $\beta$ -peptides.<sup>2</sup> Specifically, the ring constraint locks the dihedral angle  $\theta$  at around  $-90^\circ$  with which *trans*-ACPC forms a stable pseudo-diequatorial structure.<sup>36,37</sup>

This effect on dihedral angle  $\theta$  is expected to exist in  $\beta$ -peptoids consisting of *trans*-ACPC (Fig. 1c right). Bond rotation about  $\omega$  in oligo(*N*-substituted *trans*-ACPCs) was expected to be restricted (to  $\sim 180^\circ$ ) because of the steric repulsions between cyclopentane rings of neighboring residues. Moreover, the cyclopentane ring exerts steric effects on the amide bonds and *N*-substituents, which could restrict the bond rotations about  $\phi$  and  $\psi$ .

To precisely predict the low-energy conformations of oligo(*N*-substituted *trans*-ACPCs), we employed density functional theory (DFT) calculations. We first investigated the conformational landscape of acetyl-*N*-methyl-*trans*-ACPC dimethylamide (**Me1**), a minimal model of ACPC  $\beta$ -peptoids by DFT calculations in vacuo (Fig. 2a). The bonds about the dihedral angles  $\phi$  and  $\psi$  were rotated in combination with a  $15^\circ$  increment and the energy of each conformer was plotted. During the  $\phi$  and  $\psi$  scans, the dihedral angle  $\omega$  was fixed at either  $180^\circ$  or  $0^\circ$ . The dihedral angle  $\theta$  of the initial conformation was set to obtain the gauche conformation about the  $C_\alpha$ - $C_\beta$  bond according to the previous reports on  $\beta$ -peptides consisting of *trans*-ACPC.<sup>2,36,38</sup> The  $\phi$  and  $\psi$  scanning results revealed that the conformer with  $(\omega, \phi, \theta, \psi) = (180^\circ, -60^\circ, -80^\circ, 165^\circ)$  (**conformer 1**) was the most stable. In this conformer, the cyclopentane ring formed an envelope shape with a  $C_\epsilon$ -exo pucker, where the  $\epsilon$ -carbon is out of the plane in the direction toward the carbonyl carbon of the same residue (Fig. 2b left). Another stable conformer with  $(\omega, \phi, \theta, \psi) = (0^\circ, 120^\circ, -84^\circ, 150^\circ)$  (**conformer 2**) was obtained, which was 1.1 kcal/mol higher in energy than **conformer 1**. The cyclopentane ring in this conformer was found to form an envelope shape with a  $C_\gamma$ -endo pucker, where the  $\gamma$ -carbon is out of the plane in the direction toward the nitrogen of the same residue (Fig. 2b right). The values of dihedral angle  $\theta$  in the two conformers are consistent with those mentioned in previous

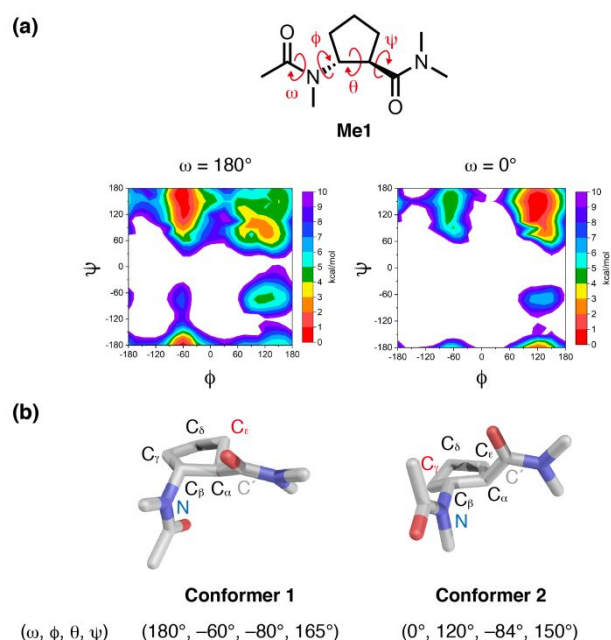


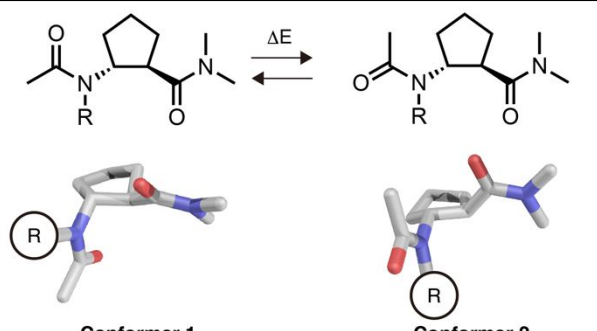
**Fig. 2** (a) Ramachandran-type plots of **Me1** with  $\omega = 180^\circ$  (left) and  $\omega = 0^\circ$  (right). Relative energy (kcal/mol) with respect to those of **conformer 1** (left) and **conformer 2** (right). Regions with relative energies over 10 kcal/mol are shown in white. (b) A stick model of the most stable conformer with  $\omega = 180^\circ$  (left) and  $\omega = 0^\circ$  (right). The backbone dihedral angles and energy difference (kcal/mol) are shown at the bottom. The definition of each dihedral angle is shown in Fig. 1c. The carbon in the ring that is off the plane is labeled in red.

reports on  $\beta$ -peptides comprising *trans*-ACPC.<sup>2,36,38</sup> **Conformers 1** and **2** were much more stable than any other conformers having the same *w* values.

Next, we evaluated the influence of the structures of *N*-substituents on the relative stabilities of the conformers. The conformations of acetylated *N*-substituted *trans*-ACPC dimethylamide with methyl (**Me1**), ethyl (**Et1**), propyl (**Pr1**), isobutyl (**Ib1**), or neopentyl (**Np1**) group as the *N*-substituent were optimized in vacuo for the two conformers (Fig. S1). The relative stability of **conformer 1** compared to **conformer 2** increased as the bulkiness of the *N*-substituent increased. Moreover, in case of **Ib1** and **Np1**, **conformer 1** was more stable than **conformer 2** by 2.1 and 4.0 kcal/mol, respectively, which indicates a strong preference for **conformer 1** over **conformer 2** in these cases (Table 1). This is probably because the *N*-substituent and the cyclopentane ring are in proximity in **conformer 2** and the increased size of the *N*-substituent produces a larger steric effect (Fig. S1). Thus, larger *N*-substituents increase the relative stability of **conformer 1** over **conformer 2**.

Based on the results of the monomer model study, we attempted to predict the three-dimensional structures of the oligo(*N*-substituted *trans*-ACPCs). The initial conformers of *N*-isobutyl ACPC dimer (**Ib2**), trimer (**Ib3**), and tetramer (**Ib4**) were built by connecting the **conformer 1** of the monomer. The geometries of **Ib2**, **Ib3**, and **Ib4** were optimized using DFT calculations in vacuo (Fig. S2). The dimer, trimer and tetramer of **conformer 1** adopted a strand shape. For comparison, another predicted dimer, trimer and tetramer structure was built by connecting **conformer 2** of the monomer. The tetramer of the less stable **conformer 2** adopted a narrow helical structure. Consistent with the results of the monomer study, the dimer, trimer, and tetramer consisting of **conformer 1** were

**Table 1.** Influence of *N*-substituent structures on relative stability of **conformers 1** and **2** of *N*-substituted *trans*-ACPC monomers.



Compound	R	$\Delta E$ (kcal/mol) <sup>a</sup>
<b>Me1</b>	Methyl	1.1
<b>Et1</b>	Ethyl	1.4
<b>Pr1</b>	Propyl	1.4
<b>Ib1</b>	Isobutyl	2.1
<b>Np1</b>	Neopentyl	4.0

<sup>a</sup>The energy difference of the molecule at **conformer 2** with the molecule at **conformer 1** in vacuo.

more stable than those consisting of **conformer 2** by 4.3, 6.7 and 9.1 kcal/mol, respectively (Fig. S2). These results suggest that oligo(*N*-isobutyl *trans*-ACPCs) forms a strand shape consisting of **conformer 1** as the most stable structure.

To experimentally validate the three-dimensional structure of **Ib4**, we synthesized the oligomer and conducted X-ray crystallographic studies. The oligomer was synthesized on solid phase using the procedures that is slightly modified from the procedures we have previously developed for  $\beta$ -peptoid synthesis (Scheme S1).<sup>39</sup> To achieve efficient coupling reaction, we explored various coupling conditions and found that COMU is effective for the coupling of Fmoc-*trans*-ACPC-OH and elevating the reaction temperature to 60 °C is required. With the modified coupling conditions, the tetramer of *N*-isobutyl *trans*-ACPCs was synthesized on solid phase with moderate yield (24%). After being cleaved from resin, the tetramer was dimethylamidated in solution to yield **Ib4**. Single crystals of **Ib4** were grown, and the X-ray diffraction pattern from a single crystal revealed the three-dimensional structure of **Ib4** (Fig. 3).

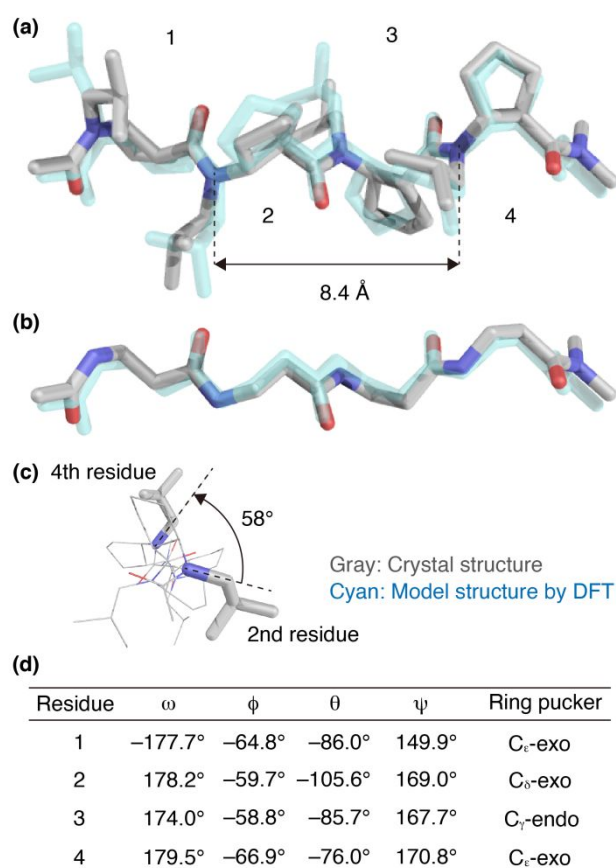


**Fig. 3** (a) Overlay of an X-ray crystal structure (gray) and a model structure by DFT calculations (cyan) of acetyl-*N*-isobutyl-*trans*-ACPC tetramer dimethylamide. The residue numbers are labeled. The distance of the *N*-substituents at 2<sup>nd</sup> and 4<sup>th</sup> residues that face the same direction is labeled. (b) Only backbone structures of (a) are shown. (c) View of the crystal structure from longitudinal direction. *N*-substituents on 2<sup>nd</sup> and 4<sup>th</sup> residues are shown in stick and other structures are shown in line. (d) Dihedral angles and ring puckering of each residue in the crystal structure.



Two molecules of **ib4** and two molecules of trifluoroacetic acid (TFA) were present in each unit cell of the crystal structure. In the crystal structure, **ib4** was found to form an extended strand-like shape, which overlapped well with the DFT-predicted structure that was built by connecting **conformer 1** of the monomer (backbone root mean square deviation or R.M.S.D. = 0.464 Å, Fig. 3a and b). All the backbone dihedral angles were within  $\pm 30^\circ$  from those in the DFT-predicted structure of **conformer 1** (Fig. 3d). This indicates that the preorganized conformation of the designed monomer was well-preserved in the oligomer structure, and the assembly of the designed preorganized monomer successfully led to a  $\beta$ -peptoid with a defined shape. The pitch of the strand was 8.4 Å and the strand was left-handedly twisted by  $58^\circ$  for every two residues (Fig. 3c). While there was a  $C_\epsilon$ -exo pucker in the model structure for all residues, the ring pucker in the crystal structure varied residue by residue (Fig. 3d). Because the envelope shape of cyclopentane is flexible, the carbon that is out of the ring plane varies. The 1st and 4th residues were  $C_\epsilon$ -exo pucker, the 2nd residue was  $C_\delta$ -exo pucker, and 3rd residue was  $C_\gamma$ -endo pucker. This suggests that some conformational freedom of ring puckering exists in the ACPC  $\beta$ -peptoids. Despite the residue-by-residue deviations of the ring pucker, backbone dihedral angle  $\theta$ , which corresponds to the rotation of a C–C bond on the cyclopentane ring, was retained at around  $-80^\circ$ , suggesting that the ring pucker does not have a strong impact on the backbone shape.

Next, we conducted an NMR study of oligo(*N*-isobutyl *trans*-ACPCs) to determine whether the oligomers maintained their twisted strand shape in solution. Because the structure of oligo(*N*-isobutyl *trans*-ACPCs) is stabilized on a per-residue basis, the shortest oligomer **ib2** was recruited as a simple model compound for NMR analysis. The one-dimensional (1D) and two-dimensional (2D) NMR spectra of **ib2** in CDCl<sub>3</sub> were recorded. The NMR spectra of **ib2** indicate there is a dominant conformation. The peaks in <sup>1</sup>H NMR spectrum (Fig. S3) corresponding to the major conformer were unambiguously assigned using HMBC, COSY, TOCSY and HSQC spectra (Fig. S4–S7 and Table S1). Information regarding the spatial proximities of the **ib2** protons was obtained by measuring the ROESY spectrum (Fig. S8). As a reference structure, we prepared the **ib2** conformation based on the crystal structure of **ib4**, wherein the two C-terminal residues were removed from **ib4** to generate a structure corresponding to **ib2**. In order to exclude the packing effect and include the effect of the solvent used in the

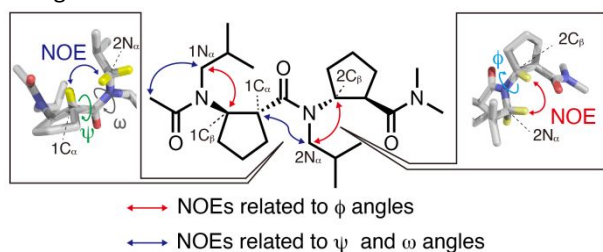


**Fig. 4** NOEs of **ib2** in CDCl<sub>3</sub>. Inter-residue cross-peaks indicating the backbone rotational restrictions observed in ROESY spectrum are shown with arrows.

solution structure analysis, the **ib2** structure was geometry-optimized using DFT calculations using chloroform as the solvent with an implicit manner (Fig. S9). The backbone conformation was not largely changed by the optimization. This suggests that the twisted strand shape of the  $\beta$ -peptoid observed in the crystal is expected to be also observed in chloroform. In fact, the information of the backbone structure obtained from the ROESY spectrum was consistent with the DFT-generated model structure (Fig. 4). First, the NOE between an  $N_\alpha$  proton and a  $C_\beta$  proton in the same residue indicates a rotational restriction about the  $\phi$  angle. Second, the NOE between an  $N_\alpha$  proton and a  $C_\alpha$  proton of the preceding residue indicates a rotational restriction about the  $\psi$  angle. The NOE also indicates that the amide bond is in the *trans*-configuration, i.e., the  $\omega$  angle is restricted to  $\sim 180^\circ$ .

The NMR spectra also showed minor peaks, suggesting the existence of minor conformers. The  $C_\alpha$ ,  $C_\beta$ , and  $N_\alpha$  protons of all

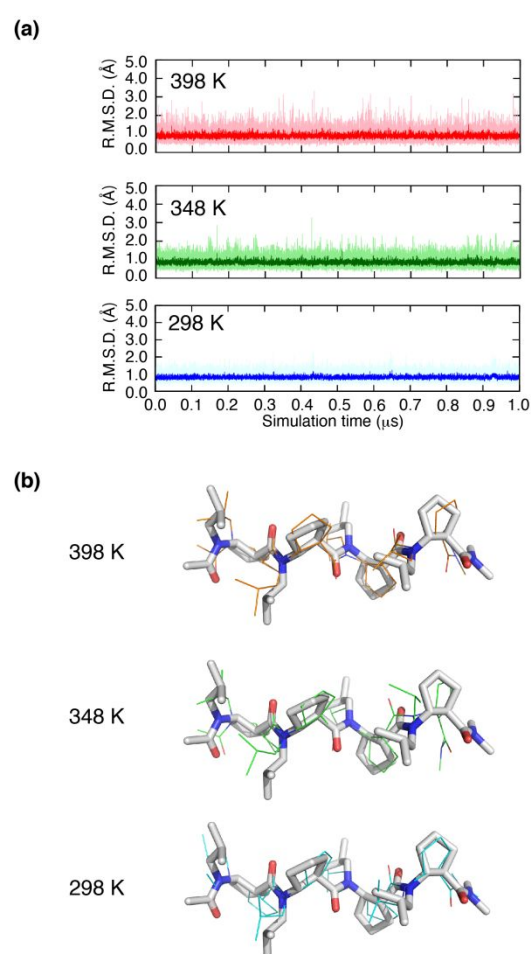


**Fig. 5** MD simulations of (**ib4**) in chloroform. (a) R.M.S.D. values of backbone atoms (N,  $C_\alpha$ ,  $C_\beta$ , C', O) in MD simulations. The mean R.M.S.D. values at 298 K (blue), 348 K (green), and 398 K (red) are shown as dark-color lines overwritten on six MD runs shown as light-color lines. (b) Conformations before (gray) and after 1  $\mu$ s MD simulation (Run 1) at 298 K (blue), 348 K (green), and 398 K (orange). The conformations after 1  $\mu$ s MD simulations of Run 2–6 are shown in Fig. S12.

the conformers were assigned in a similar manner as the assignment of protons on the major conformers (Table S1). Three sets of minor peaks were observed in the spectra, and the ROESY spectrum suggests that each of them has one or two *cis* amides (Fig. S10). The abundance of the three minor conformers was 23% of the total population according to the HSQC spectrum (Fig. S11).

The NMR results suggest that ACPC oligomers predominantly form a strand shape in solution, as observed in the DFT calculations and the crystal structure.

Finally, to assess the conformational dynamics of the twisted strand shape of oligo(*N*-isobutyl *trans*-ACPCs), MD simulations of **1b4** in chloroform were performed. Six runs of 1  $\mu$ s simulations were conducted at 298, 348, and 398 K. The crystal structure was set as the initial conformation for simulations. The strand shape was maintained at all the tested temperatures (298, 348, and 398 K) throughout the simulation time (Fig. 5a). As shown in Fig. 5b, the initial conformation of **1b4** was maintained after the 1  $\mu$ s simulations at 298, 348 and 398 K (Fig. 5b and Fig. S12). This result supports the strong preference of **conformer 1** for **1b4** indicated by the results of DFT calculations and the NMR studies. The dihedral angle  $\chi_N$ , which determines the orientation of the *N*-substituents (Fig. S1), was also restricted to approximately 60°–120° at 298 K, although it occasionally flipped by approximately 180°. The rotational restrictions were presumably caused by the steric repulsions between the *N*-substituent, backbone atoms, and other *N*-substituents. The rotational freedom of the  $\chi_N$  angles were increased upon increasing the temperature to 348 K and 398 K (Fig. S13).

## Conclusions

In conclusion, we have reported a  $\beta$ -peptoid with an extended three-dimensional structure. The monomer structure was shown to be preorganized via the interplay of the backbone cyclopentane ring and *N*-substituents. The conformation of *N*-isobutyl *trans*-ACPC oligomers observed in the crystal structure and in solution was consistent with the most stable conformation predicted from the DFT calculations. This design shown here successfully led to the first per-residue restrictions of all four backbone dihedral angles of  $\beta$ -peptoids. We envision that the monomers with different cyclic constraints, such as 2-aminocyclohexanecarboxylic acid, would provide other preorganized monomers with defined shapes. Such peptoid monomers would accelerate de novo design of more diverse peptoid-type oligomers with defined shapes. These oligomers will be useful as scaffolds for designing functional molecules such as catalysts<sup>40</sup> and protein ligands.<sup>27,41–43</sup>

## Author Contributions

J. K. synthesized compounds, DFT calculations, conducted X-ray crystallographic analysis, and wrote the original draft of the manuscript. H. K. and Y. S. synthesized compounds. M. Y. conducted DFT calculations. T. U. and K. Takeuchi conducted NMR spectroscopic

analysis. K. U. and D. K. performed molecular dynamics simulations. K. Tsumoto supervised the part of the work. J. M. conceived the idea, supervised the work, synthesized compounds, and wrote the original draft of the manuscript. S. S. supervised the work, wrote the original draft of the manuscript. All the authors contributed review and editing of the manuscript.

## Conflicts of interest

The authors declare the following competing financial interest: The authors (J.M. and S.S.) have filed a patent application (PCT/JP2020/27010).

## Acknowledgements

We thank Dr. Y. Kohuku at the University of Tokyo and Dr. I. Shimada at RIKEN Center for Biosystems Dynamics Research for NMR measurements using high magnetic field NMR spectrometers. S.S. and K.U. acknowledge financial support from CREST (JPMJCR21N5), Japan Science and Technology Agency. J.M. acknowledges financial support from PREST (JPMJPR21AF), Japan Science and Technology Agency. D.K. acknowledges financial support from JSPS KAKENHI (21K18310 and 19H04202) and AMED (JP20wm0325002). K.T. acknowledges financial support from CREST (JPMJCR20H8), Japan Science and Technology Agency. T. Ueda acknowledges financial support from MEXT/JSPS KAKENHI (JP21H05509, JP20H03375, and JP17H06097). K. Takeuchi acknowledges financial support from JSPS KAKENHI (JP20K21494 and JP20H03378). The computation was performed using Research Center for Computational, Science, Okazaki, Japan (Project: 22-IMS-C079). We thank Drs. S. Kusumoto and T. Iwasaki at the University of Tokyo for the assistance on solving the X-ray crystal structure. The X-ray diffraction data of the crystal were collected using an instrument at Advanced Characterization Nanotechnology Platform of the University of Tokyo, supported by “Nanotechnology Platform” of the Ministry of Education, Culture, Sports, Science and Technology (MEXT), Japan.

## Notes and references

- 1 D. H. Appella, L. A. Christianson, I. L. Karle, D. R. Powell and S. H. Gellman, *J. Am. Chem. Soc.*, 1996, **118**, 13071–13072.
- 2 D. H. Appella, L. A. Christianson, D. A. Klein, D. R. Powell, X. Huang, J. J. Barchi and S. H. Gellman, *Nature*, 1997, **387**, 381–384.
- 3 B. A. F. Le Bailly and J. Clayden, *Chem. Commun.*, 2016, **52**, 4852–4863.
- 4 V. Berl, I. Huc, R. G. Khoury, M. J. Krische and J.-M. Lehn, *Nature*, 2000, **407**, 720–723.
- 5 I. Huc, *J. Am. Chem. Soc.*, 2003, **125**, 3448–3449.
- 6 G. Guichard and I. Huc, *Chem. Commun.*, 2011, **47**, 5933–5941.
- 7 P. Teng, N. Ma, D. C. Cerrato, F. She, T. Odom, X. Wang, L.-J. Ming, A. van der Vaart, L. Wojtas, H. Xu and J. Cai, *J. Am. Chem. Soc.*, 2017, **139**, 7363–7369.

- 8 F. She, P. Teng, A. Peguero-Tejada, M. Wang, N. Ma, T. Odom, M. Zhou, E. Gjonaj, L. Wojtas, A. van der Vaart and J. Cai, *Angew. Chem. Int. Ed.*, 2018, **57**, 9916–9920.
- 9 Y. Shi, P. Teng, P. Sang, F. She, L. Wei and J. Cai, *Acc. Chem. Res.*, 2016, **49**, 428–441.
- 10 R. J. Simon, R. S. Kania, R. N. Zuckermann, V. D. Huebner, D. A. Jewell, S. Banville, S. Ng, L. Wang, S. Rosenberg, C. K. Marlowe, D. C. Spellmeyer, R. Tan, A. D. Frankel, D. V. Santi, F. E. Cohen and P. A. Bartlett, *Proc. Natl. Acad. Sci. U. S. A.*, 1992, **89**, 9367–9371.
- 11 N. H. Shah, G. L. Butterfoss, K. Nguyen, B. Yoo, R. Bonneau, D. L. Rabenstein and K. Kirshenbaum, *J. Am. Chem. Soc.*, 2008, **130**, 16622–16632.
- 12 D. Gimenez, J. A. Aguilar, E. H. C. Bromley and S. L. Cobb, *Angew. Chem. Int. Ed.*, 2018, **57**, 10549–10553.
- 13 C. Caumes, O. Roy, S. Faure and C. Taillefumier, *J. Am. Chem. Soc.*, 2012, **134**, 9553–9556.
- 14 A. W. Wijaya, A. I. Nguyen, L. T. Roe, G. L. Butterfoss, R. K. Spencer, N. K. Li and R. N. Zuckermann, *J. Am. Chem. Soc.*, 2019, **141**, 19436–19447.
- 15 P. Armand, K. Kirshenbaum, R. A. Goldsmith, S. Farr-Jones, A. E. Barron, K. T. V. Truong, K. A. Dill, D. F. Mierke, F. E. Cohen, R. N. Zuckermann and E. K. Bradley, *Proc. Natl. Acad. Sci. U. S. A.*, 1998, **95**, 4309–4314.
- 16 J. R. Stringer, J. A. Crapster, I. A. Guzei and H. E. Blackwell, *J. Am. Chem. Soc.*, 2011, **133**, 15559–15567.
- 17 R. Shyam, L. Nauton, G. Angelici, O. Roy, C. Taillefumier and S. Faure, *Biopolymers*, 2019, **110**, e23273.
- 18 C. M. Davern, B. D. Lowe, A. Rosfi, E. A. Ison and C. Proulx, *Chem. Sci.*, 2021, **12**, 8401–8410.
- 19 M. Pypec, L. Jouffret, C. Taillefumier and O. Roy, *Beilstein J. Org. Chem.*, 2022, **18**, 845–854.
- 20 D. Gimenez, G. Zhou, M. F. D. Hurley, J. A. Aguilar, V. A. Voelz and S. L. Cobb, *J. Am. Chem. Soc.*, 2019, **141**, 3430–3434.
- 21 O. Roy, G. Dumonteil, S. Faure, L. Jouffret, A. Kriznik and C. Taillefumier, *J. Am. Chem. Soc.*, 2017, **139**, 13533–13540.
- 22 J. A. Crapster, I. A. Guzei and H. E. Blackwell, *Angew. Chem. Int. Ed.*, 2013, **52**, 5079–5084.
- 23 K. Huang, C. W. Wu, T. J. Sanborn, J. A. Patch, K. Kirshenbaum, R. N. Zuckermann, A. E. Barron and I. Radhakrishnan, *J. Am. Chem. Soc.*, 2006, **128**, 1733–8.
- 24 R. V. Mannige, T. K. Haxton, C. Proulx, E. J. Robertson, A. Battigelli, G. L. Butterfoss, R. N. Zuckermann and S. Whitelam, *Nature*, 2015, **526**, 415–420.
- 25 B. C. Gorske, E. M. Mumford and R. R. Conry, *Org. Lett.*, 2016, **18**, 2780–2783.
- 26 B. C. Gorske, E. M. Mumford, C. G. Gerrity and I. Ko, *J. Am. Chem. Soc.*, 2017, **139**, 8070–8073.
- 27 J. Morimoto, Y. Fukuda, D. Kuroda, T. Watanabe, F. Yoshida, M. Asada, T. Nakamura, A. Senoo, S. Nagatoishi, K. Tsumoto and S. Sando, *J. Am. Chem. Soc.*, 2019, **141**, 14612–14623.
- 28 Y. Fukuda, M. Yokomine, D. Kuroda, K. Tsumoto, J. Morimoto and S. Sando, *Chem. Sci.*, 2021, **12**, 13292–13300.
- 29 M. Yokomine, J. Morimoto, Y. Fukuda, Y. Shiratori, D. Kuroda, T. Ueda, K. Takeuchi, K. Tsumoto and S. Sando, *Angew. Chem. Int. Ed.*, 2022, **61**, e202200119.
- 30 B. C. Hamper, S. A. Kolodziej, A. M. Scates, R. G. Smith and E. Cortez, *J. Org. Chem.*, 1998, **63**, 708–718.
- 31 A. S. Norgren, S. Zhang and P. I. Arvidsson, *Org. Lett.*, 2006, **8**, 4533–4536.
- 32 C. A. Olsen, M. Lambert, M. Witt, H. Franzyk and J. W. Jaroszewski, *Amino Acids*, 2008, **34**, 465–471.
- 33 K. J. Lee, W. S. Lee, H. Yun, Y. J. Hyun, C. D. Seo, C. W. Lee and H. S. Lim, *Org. Lett.*, 2016, **18**, 3678–3681.
- 34 J. S. Laursen, P. Harris, P. Fristrup and C. A. Olsen, *Nat. Commun.*, 2015, **6**, 7013.
- 35 J. Morimoto, J. Kim, D. Kuroda, S. Nagatoishi, K. Tsumoto and S. Sando, *J. Am. Chem. Soc.*, 2020, **142**, 2277–2284.
- 36 J. Applequist, K. A. Bode, D. H. Appella, L. A. Christianson and S. H. Gellman, *J. Am. Chem. Soc.*, 1998, **120**, 4891–4892.
- 37 L. A. Christianson, M. J. Lucero, D. H. Appella, D. A. Klein and S. H. Gellman, *J. Comput. Chem.*, 2000, **21**, 763–773.
- 38 D. H. Appella, L. A. Christianson, D. A. Klein, M. R. Richards, D. R. Powell and S. H. Gellman, *J. Am. Chem. Soc.*, 1999, **121**, 7574–7581.
- 39 J. Morimoto, Y. Fukuda and S. Sando, *Org. Lett.*, 2017, **19**, 5912–5915.
- 40 Z. C. Girvin and S. H. Gellman, *J. Am. Chem. Soc.*, 2020, **142**, 17211–17223.
- 41 J. W. Checco and S. H. Gellman, *Curr. Opin. Struct. Biol.*, 2016, **39**, 96–105.
- 42 P. Sang, Y. Shi, B. Huang, S. Xue, T. Odom and J. Cai, *Acc. Chem. Res.*, 2020, **53**, 2425–2442.
- 43 J. A. Schneider, T. W. Craven, A. C. Kasper, C. Yun, M. Haugbro, E. M. Briggs, V. Svetlov, E. Nudler, H. Knaut, R. Bonneau, M. J. Garabedian, K. Kirshenbaum and S. K. Logan, *Nat. Commun.*, 2018, **9**, 4396.